

## ORIGINAL RESEARCH ARTICLE

# Sapindus emarginatus extract embedded with gold nanoparticles: An antiproliferative agent against MCF7 breast cancer cell line

S Vignesh Kumar<sup>1\*</sup>, V Kavimani<sup>2</sup>

<sup>1</sup> Department of Biotechnology, Anna University Regional Centre, Coimbatore, India. E-mail: svigneshkum6@gmail.com

<sup>2</sup> Department of Mechanical Engineering, Anna University Regional Centre, Coimbatore, India

---

### ABSTRACT

There are numerous studies reported on the usage of the sapindus emarginatus (SE) fruit in cancer and other treatments in the past few years. In this study, crude SE fruit extract was prepared and it was further used to synthesis gold nanoparticles (Au Nps). The synthesized Au Nps were left embedded in the SE fruit extract. The Au Nps embedded in the SE fruit extract (SE-Au Nps) were characterized using UV-Visible Spectroscopy, Centrifugal Particle Size analyzer (CPS), Scanning Electron Microscope (SEM) and Fourier Transform Infrared Spectroscopy (FTIR). MTT assay was carried out for both SE fruit extract and SE-Au Nps on MCF7 breast cancer cell line and thus compared. The UV-Visible Absorbance for the SE-Au Nps was obtained at 543 nm. The centrifugal particle size analysis of the Au Nps embedded in SE fruit extract showed the size of the nanoparticles to be widely varying with higher fraction of particles between the size ranges of 15 to 20 nm. The morphology of the Au Nps embedded in SE fruit extract was observed using SEM. The presence of Au Nps in SE fruit extract was confirmed using FTIR. The results of the MTT assay on MCF7 breast cancer cell line proved that the % cell viability was less for SE-Au Nps than that of the SE fruit extract alone. Thus, the antiproliferative activity of the SE fruit extract was significantly enhanced by embedding it with Au Nps and it can be effectively used in therapeutic applications after further studies.

**Keywords:** Gold Nanoparticles; Sapindus Emarginatus; Antiproliferative; MCF7

---

### ARTICLE INFO

Received: 25 March 2021  
Accepted: 11 May 2021  
Available online: 18 May 2021

### COPYRIGHT

Copyright © 2021 S Vignesh Kumar, et al. EnPress Publisher LLC. This work is licensed under the Creative Commons Attribution-NonCommercial 4.0 International License (CC BY-NC 4.0).  
<https://creativecommons.org/licenses/by-nc/4.0/>

## 1. Introduction

Cancer is the abnormal growth of cells with uncontrolled division resulting in increased number of cells<sup>[1]</sup>. Cancer is observed as the most dangerous class of disease categorized by uncontrolled cell growth<sup>[2,3]</sup>. There is a marginal increase in cancer cases in the last few years, and most of the time, it ends up with taking life<sup>[4,5]</sup>. Breast cancer is a complex and heterogeneous disease<sup>[6]</sup>. In world, breast cancer represents 9% of the global cancer burden and is the third most common tumour. Human breast cancer MCF7 cells represent one of the most widely used experimental models for *in vitro* studies on breast carcinoma<sup>[7]</sup>.

A considerable part of the current knowledge on breast carcinomas is based on *in vivo* and *in vitro* studies performed with cell lines derived from breast cancer. In reference to the treatments available for cancer, the characteristics of the cancer determine the treatment, which may include surgery, medications (hormonal therapy and chemotherapy), radiotherapy and immunotherapy. There are currently three main

groups of medications for breast cancer, such as hormone blocking agents (Tamoxifen, Anastrozole or Letrozole), chemotherapy (cyclophosphamide, methotrexate and fluorouracil) and monoclonal antibodies (Trastuzumab). Radiotherapy is given after surgery to the region of the tumor bed and regional lymph nodes, to destroy microscopic tumor cells that may have escaped surgery. Radiation can reduce the risk of recurrence by 50%–60%<sup>[8]</sup>. Most chemotherapy medications work by destroying fast-growing and/or fast-replicating cancer cells, either by causing DNA damage upon replication or by other mechanisms. Along with the medications chemotherapy and radiation can also affect healthy cells. For example, damage to the heart muscle is the most dangerous complication of doxorubicin. Trastuzumab is very expensive and its use may cause serious side effects (approximately 2% of patients who receive it suffer from significant heart damage). Due to growing resistance and side effects to these therapies search for new therapeutics for breast cancer has become essential. Scientific interest in medicinal plant has bloomed in recent times due to increased efficiency of new plant derived drugs and wide spread concerns about the side effects of modern medicine<sup>[9]</sup>.

*Sapindus emarginatus* Vahl found in South India is commonly known as soap nut tree. The tree species is inadequately distributed in diverse geographical provinces like Gangetic plains, Western Ghats and Deccan Plateau in India<sup>[10]</sup>. The genus *Sapindus* possesses tremendous medicinal value. Since past, it is used as emetic, tonic, astringent, anthelmintic, for asthma, colic, diarrhea, cholera, tubercular glands and paralysis of limbs. Methanolic extract of fruit of *Sapindus emarginatus* (SE) found to produce CNS depressant activity<sup>[11]</sup>. The fruits are usually used for hair problems and also in preparation of shampoos. Traditionally SE is used as anti-inflammatory and antipruritic medicine. The seed is an intoxicant and the fruit rind has oxytropic action. Its powder is used as nasal insufflations<sup>[12]</sup>. Saponins isolated from different plants and animals have been shown to specifically inhibit the growth of cancer cells *in vitro*<sup>[13–18]</sup>. The saponins from SE fruit extract found to have significant antihyperlipidemic activity<sup>[19]</sup>.

The combined application of saponins with other antitumor compounds may increase cytotoxic activity of the latter, which is an interesting new possibility in cancer treatment research<sup>[20]</sup>. The noble metal nanoparticles like gold nanoparticles represent smart and promising candidates in the drug delivery applications due to their unique dimensions, tunable functionalities on the surface, and controlled drug release<sup>[21]</sup>. Another essential aspect while working with Au NP in bio-applications is safety and biocompatibility (Au NP is already approved by the US Food and Drug Administration.) Biologically synthesized and functionalized, Au NP provides many desirable attributes for use as carriers in drug delivery systems as the functionalized Au NP core is essentially inert and nontoxic reported in recent studies<sup>[22]</sup>. The labeling of AuNPs with biological ligands to specifically bind to desired cancer cells increases the effectiveness of thermal energy transfer to cancer cells without harming non-cancerous cells<sup>[23]</sup>. After cellular uptake, the Au Nps can act as tiny, precise and powerful heaters (thermal scalpels) to kill cancer and they are capable of inducing apoptosis in B-chronic lymphocytic leukemia<sup>[24]</sup>.

It has been found that gold nanoparticles embedded in *Rubia cordifolia* (RC) matrix significantly enhanced anti-inflammatory characteristics by inhibiting nitric oxide release<sup>[25]</sup>. It was reported in terms of inhibitory concentration for 50% inhibition compared to either RC extract or Au NPs. Hence, in this work the SE fruit extract was embedded with gold nanoparticles with the vision of increasing its anti-proliferative activity.

## 2. Materials and methods

### 2.1 Preparation of plant extract

Fresh fruits of SE were collected from the nursery of Institute of Forest Genetics and Tree Breeding (IFGTB), Coimbatore, Tamilnadu. Collected SE fruits were dried under shade, mechanically powdered and stored in an airtight container. Dried and powdered SE fruits were extracted with 95% methanol in a Soxhlet extractor. The methanolic extract was concentrated to give a dark brown residue which

was partitioned between water-n-Butanol (1:1). The n-butanolic layer was evaporated to give the crude saponin fraction as a brown residue<sup>[26]</sup>.

## 2.2 Synthesis of gold nanoparticles (Au NPs) embedded in SE fruit extract (SE-AU NPs)

A solution of 50 ml, 0.001 M (0.39382 mg/ml) gold (III) chloride trihydrate ( $\text{HAuCl}_4 \cdot 3\text{H}_2\text{O}$ ) and 50 ml SE fruit extract, diluted in 50 ml of distilled water, was added together drop by drop and stirred on a magnetic stirrer. The solution was ultrasonicated at a high frequency of 10 KHz for 3 h and then maintained at a stationary position for 2 h at room temperature.

## 2.3 Characterization of SE-AU NPs

SE-Au Nps were characterized by UV-Visible Absorption Spectroscopy, Centrifugal Particle Size analyzer (CPS), Fourier Transform Infrared Spectroscopy (FTIR) and a Scanning Electron Microscope (SEM).

## 2.4 UV-Visible Absorbance Spectroscopy studies

UV-Visible Absorbance Spectroscopy have been proved to be quite sensitive to the formation of gold colloids because gold nanoparticles exhibit an intense absorption peak around 540 nm due to the surface plasmon (it describes the collective excitation of conduction electrons in a metal) excitation. The sample was analyzed using UV-9000S Spectrophotometer (Lark, India). Distilled water was used as a blank.

### CPS

The gold nanoparticles embedded in the plant extract were isolated by centrifugation. Diluted suspensions of sucrose, on the order of 0.01–1.0 [wt%], were prepared. The sugar solution and our sample solutions were injected in disc centrifuge. Nanoparticle size was analyzed by injection of 350  $\mu\text{l}$  of sample into CPS operating at a speed of 20,000 rpm. All analyses were run against a known calibration standard and the particles in the solution were analyzed by size distribution graph.

### SEM

Morphology of the synthesized Au Nps in the SE fruit extract was analyzed using SEM. Few drops of the SE fruit extract embedded with the Au Nps was spread on a cover slip and dried. Then the sample on the cover slip was coated with gold in a sputter coating unit for few minutes.

### FTIR

The samples were completely dissolved in respective solvents, non-sticky and the pH was found to be less than 8 which are necessary conditions to analyze the liquid samples. The sample analysis was carried out using FTIR (Brucker–Tensor 27) in ATR mode with a range from 500 to 4000  $\text{cm}^{-1}$ . The liquid samples are directly placed onto the ZnSe crystal to obtain the spectrum.

## 3. Cell proliferation assay on MCF7 cell line

### 3.1 Chemicals and reagents

MTT (3-[4,5-dimethylthiazol-2-yl]-2,5-diphenyl tetrazolium bromide) Invitrogen, USA. Acridine orange was obtained from Sigma, USA. All other fine chemicals were obtained from Sigma–Aldrich, St. Louis.

### 3.2 Cell culture

MCF7 cells obtained from NCCS (National Centre for Cell Science, Pune) were cultured in Rose well Park Memorial Institute medium (RPMI), supplemented with 10% fetal bovine serum, penicillin/streptomycin (250 U/ml), gentamycin (100  $\mu\text{g}/\text{ml}$ ) and amphotericin B (1 mg/ml) were obtained from Sigma Chemicals, MO, USA. All cell cultures were maintained at 37 °C in a humidified atmosphere of 5%  $\text{CO}_2$ . Cells were allowed to grow to confluence over 24 h before use.

## 4. Cell growth inhibition studies by MTT assay

Cell viability was measured with the conventional MTT reduction assay, as described previously with slight modification. Briefly, MCF7 cells were

seeded at a density of  $5 \times 10^3$  cells/well in 96-well plates for 24 h, in 200  $\mu$ l of RPMI with 10% FBS. Then culture supernatant was removed and RPMI containing various concentrations (0.11–100  $\mu$ g/ml) of test compound was added and incubated for 48 h. After treatment, cells were incubated with MTT (10  $\mu$ l, 5 mg/ml) at 37 °C for 4 h and then with DMSO at room temperature for 1 h. The plates were read at 595 nm on a scanning multi-well spectrophotometer. Data represented the mean values for six independent experiments<sup>[27]</sup>. Cell viability (%) = (Mean OD/Control OD)  $\times$  100.

## 5. Results and discussion

### 5.1 Preparation of SE fruit extract

Crude extract of SE fruits was obtained as brown colored mixture from the Soxhlet apparatus. The mixture was separated into upper phase (butanol and crude saponin) and lower phase. The upper phase was evaporated and the crude saponin obtained was brown in color with a colorless lower phase.

### 5.2 Synthesis of SE-AU NP

The change in the brown color of SE fruit extract into purple color after its treatment with  $\text{HAuCl}_4 \cdot 3\text{H}_2\text{O}$  solution clearly indicated the formation of Au Nps. The color change was observed within 1 h in room temperature. Jannathul Firdhouse and Lalitha have earlier reported the similar color change as the indicator for the formation of Au Nps<sup>[28]</sup>. The reduction of metal ions was roughly monitored by visual inspection as described earlier<sup>[29]</sup>. The process performed simply at room temperature is comparatively free of toxic chemical hazards.

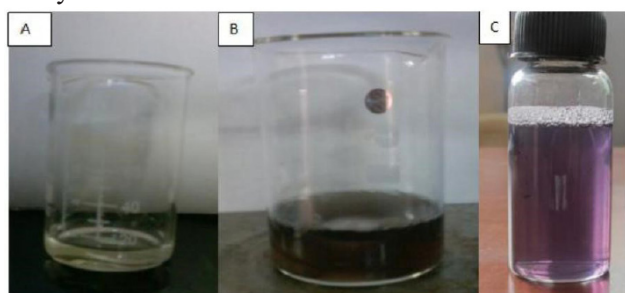


**Figure 1.** Synthesized Au Np. (A)  $\text{HAuCl}_4 \cdot 3\text{H}_2\text{O}$ ; (B) Plant Extract +  $\text{HAuCl}_4 \cdot 3\text{H}_2\text{O}$ ; (C) SE-Au NP.

### 5.3 Characterization of SE-Au Nps UV-Visible Spectroscopy

The UV-Visible Absorbance for the SE-Au Nps was obtained at 543 nm and it is due to the excitation of surface plasmon vibrations in the gold nanoparticles. The spectra are consistent with previous experimental results. Parida *et al.* reported the synthesis of gold nanoparticles using *Allium cepa* extract as the reducing agent and the absorption peak was broad and found at 540 nm which might be due to polydispersity nature of the nanoparticles<sup>[30]</sup>.

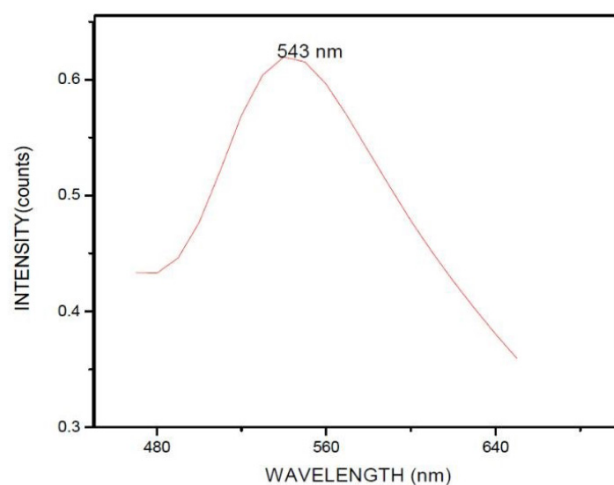


**Figure 2.** UV-Visible Spectroscopy for SE-Au NPs.

### CPS

The particle size analyzer (**Figure 3**) showed various diameter ranges of nanoparticles. The diameter versus % fraction was plotted. The size of the Au Nps embedded in SE fruit extract was found to be widely varying with higher fraction of particles between the size ranges of 15 to 20 nm.

The particle size analyzer displayed a total weight of injected gold sample as 57.26  $\mu$ g. In the injected sample 20 to 15.9 nm diameter of particles are present in high level whereas the 15.9 to 12.7 nm sized particles were in minimum level. This variation may be due to the aggregation of the nanoparticles in the extract.

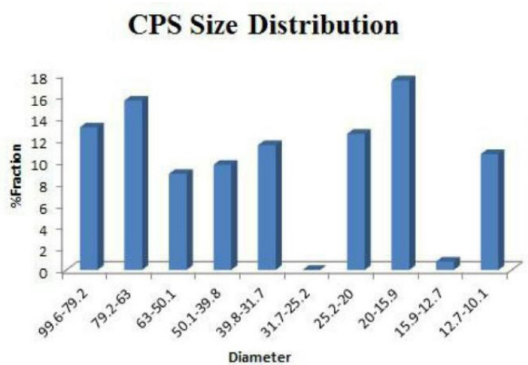


Figure 3. Particle size distribution of Au NPs.

## SEM

The SEM image (Figure 4) of SE-Au Nps showed the Au Nps distributed over the extract. The Au Nps embedded in the SE fruit extract were found to be aggregated and was not clear. The result obtained was similar to that of Paz Elia *et al.* who observed the morphology of Au Nps using plant extracts as reducing agents<sup>[31]</sup>.

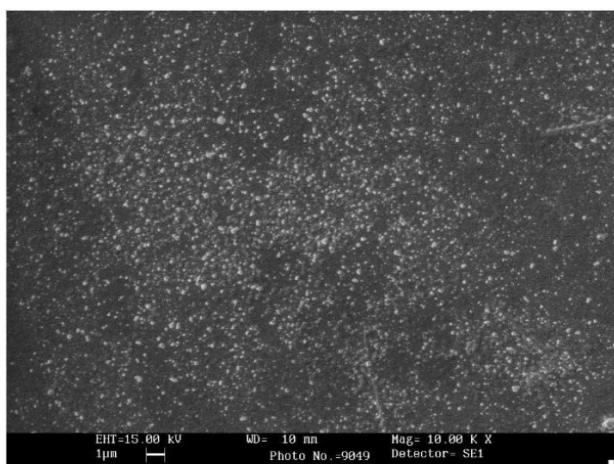


Figure 4. SEM image of SE-Au Nps.

## FTIR

FTIR spectrum of methanolic fruit extract of SE showed characteristic peaks for several functional groups like hydroxyl group in the range 3500 to 3000, C-O-C in the range of 1500 to 1000 and C-Br (alkyl) in the range of 1000 to 500. For SE-Au Nps the peak in the range of 3500 to 3000 indicates the presence of -NH<sub>2</sub> (amino) group, C-H group at 2119 and carbonyl group C=O in the range of 2000 to 2500. By comparing the spectrum of SE-Au Nps with the spectrum of SE fruit extract and the stan-

ard spectrum of gold nanoparticles<sup>[32]</sup>, it is clear that the spectra of SE embedded with gold nanoparticles indicates the presence of both the extract and the gold nanoparticle in it.

## 6. Cell proliferative study—MTT assay

The antiproliferative activity of SE fruit extract and SE-Au Nps under in vitro conditions were examined on cell proliferation by the MTT assay. MCF-7 cells were exposed to the two samples at varying concentrations for 48 h and cytotoxicity was determined using MTT assays. MTT results have shown that as the concentration of the samples increase, increased cytotoxicity was observed in a dose-dependent manner. In MTT assay, cell viability was significantly reduced to 47, 60 and 81.9% for the concentrations of 100, 10 and 1 µg respectively for SE-Au Nps and 69.9, 85.76 and 90% for 100, 10 and 1 µg respectively for crude SE fruit extract (Figure 7). The SE-AU Nps was found to be more effective compared to the crude SE fruit extract alone which indicates that Au Nps increases the cytotoxicity and has great potential as conjugate with the fruit extract and can be effectively used as anticancer agent.

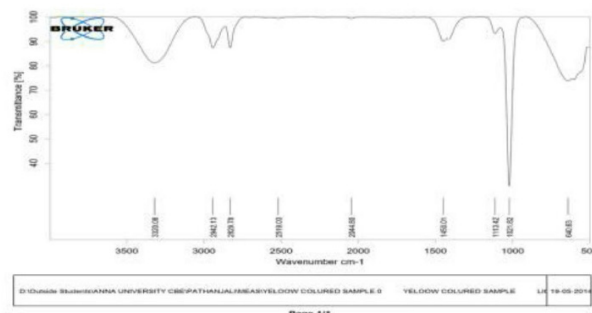


Figure 5. FTIR of SE fruit extract.

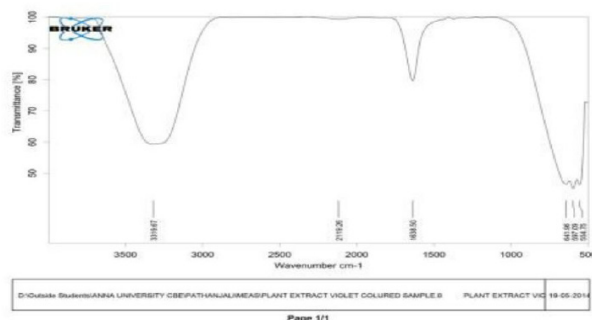


Figure 6. FTIR of SE-Au Nps.

**Table 1.** MTT assay for cell viability

Concentration	Cell viability (%)	
	Sample A	Sample B
100 $\mu$ g	47.38003	69.93933
10 $\mu$ g	60.28682	85.76944
1 $\mu$ g	81.9636	90.12686
100 ng	98.78654	95.58742
1 ng	97.90403	98.67632

## 7. Conclusion

The SE fruit extract was prepared using the soxhlet apparatus. The SE fruit extract was used to synthesize the gold nanoparticles. The synthesized gold nanoparticles embedded in the SE fruit extract (SE-Au Nps) were confirmed by its absorbance at 543 nm using the UV Vis spectrophotometer. The size of the Au Nps was found to be widely varying with higher fraction of particles between the size ranges of 15 to 20 nm. This may be due to the agglomeration of the particles. Morphology of the SE-Au Nps was observed using SEM. The FTIR analysis of the SE-Au Nps confirmed the presence of gold nanoparticles in the extract. MTT assay was carried out for both SE fruit extract and SE-Au Nps on MCF7 breast cancer cell line and compared. The results of the MTT assay on MCF7 breast cancer cell line proved that the % cell viability was less for SE-Au Nps than that of the SE fruit extract alone. Thus, the antiproliferative activity of the SE fruit extract was significantly enhanced by embedding it with Au Nps and it can be effectively used in therapeutic applications after further studies. The SE-Au Nps can be further taken to in vivo studies and then to clinical applications.

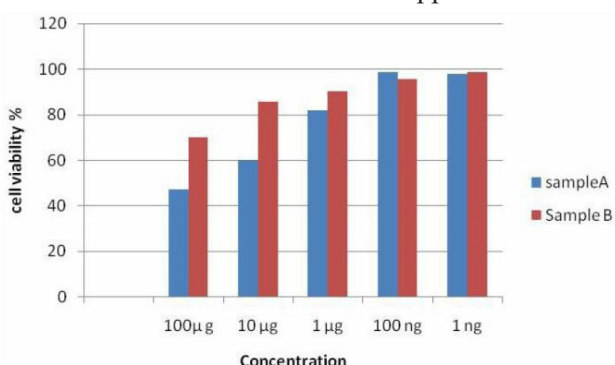


**Figure 7.** Cell viability determined by MTT assay. Sample A: SE-Au Nps. Sample B: SE fruit extract.

## Conflict of interest

No conflict of interest was reported by the authors.

## References

1. Manoharan S, Palanimuthu D, Baskaran N, *et al.* Modulating effect of lupeol on the expression pattern of apoptotic markers in 7, 12-dimethylbenz (a) anthracene induced oral carcinogenesis. *Asian Pacific Journal of Cancer Prevention* 2012; 13(11): 5753–5757.
2. Chow AY. Cell cycle control by oncogenes and tumor suppressors: Driving the transformation of normal cells into cancerous cells. *Nature Education* 2010; 3(9): 7.
3. Suriamoorthy P, Zhang X, Hao G, *et al.* Folic acid-CdTe quantum dot conjugates and their applications for cancer cell targeting. *Cancer Nano* 2010; 1: 19–28.
4. Dite GS, Whittemore A, Knight JA, *et al.* Increased cancer risks for relatives of very early-onset breast cancer cases with and without BRCA1 and BRCA2 mutations. *British Journal of Cancer* 2010; 103: 1103–1108.
5. Parveen S, Sahoo SK. Evaluation of cytotoxicity and mechanism of apoptosis of doxorubicin using folate-decorated chitosan nanoparticles for targeted delivery to retinoblastoma. *Cancer Nano* 2010; 1(1): 47–62.
6. Holliday DL, Speirs V. Choosing the right cell line for breast cancer research. *Breast Cancer Research* 2011; 13: 215.
7. Selim ME, Hendi AA. Gold nanoparticles induce apoptosis in MCF-7 human breast cancer cells. *Asian Pacific Journal of Cancer Prevention* 2012; 13(4): 1617–1620.
8. Florescu A, Amir E, Bouganim N, *et al.* Immune therapy for breast cancer in 2010 — Hype or hope? *Current oncology* 2011; 18(1): 9–18.
9. Parekh J, Chanda S. In vitro antibacterial activity of the crude methanol extract of *Woodfordia fruticosa* Kurz. Flower (Lythraceae). *Brazilian Journal of Microbiology* 2007; 38: 204–207.

10. Mahar KS, Rana TS, Ranade SA, *et al.* Genetic variability and population structure in *Sapindus emarginatus* Vahl from India. *Gene* 2011; 485(1): 32–9.
11. Chattopadhyay D, Arunachalam G, Mandal SC, *et al.* CNS activity of *Mallotus peltatus* (Geist) Muell Arg. leaf: An ethnomedicine of Onge. *Journal of Ethnopharmacology* 2003; 85(1): 99–105.
12. Nair R, Kalariya T, Chanda S. Antibacterial activity of some selected Indian medicinal flora. *Turkish Journal of Biology* 2005; 29: 41–47.
13. Kuznetzova TA, Anisimov MM, Popov AM. A comparative study in vitro of physiological activity of triterpene glycosides of marine invertebrates of echinoderm type. *Comparative Biochemistry and Physiology* 1982; 73C: 41–43.
14. Rao AV, Sung MK. Saponins as anticarcinogens. *Journal of Nutrition* 1995; 125: 717S–724S.
15. Konoshima T, Takasaki M, Tokuda H, *et al.* Anti-tumor-promoting activity of majonoside-R2 from Vietnamese ginseng, *Panax vietnamensis* HA et GRUSHV. (I). *Biological and Pharmaceutical Bulletin* 1998; 21: 834–838.
16. Marino SD, Iorizzi M, Palagiano E, *et al.* Starfish saponins. 55. Isolation, structure elucidation, and biological activity of steroid oligoglycosides from an Antarctic starfish of the family Asteriidae. *Journal of Natural Products* 1998; 61: 1319–1327.
17. Mimaki Y, Kuroda M, Kameyama A, *et al.* Steroidal saponins from the underground parts of *Ruscus aculeatus* and their cytostatic activity on HL-60 cells. *Phytochemistry* 1998; 48: 485–493.
18. Podolak I, Elas M, Cieszka K. *In vitro* antifungal and cytotoxic activity of triterpene saponosides and quinoid pigments from *Lysimachia vulgaris* L. *Phytotherapy Research* 1998; 12: S70–S73.
19. Jeyabalan S, Palayan M. Antihyperlipidemic activity of *Sapindus emarginatus* in Triton WR-1339 induced albino rats. *Research Journal of Pharmacy and Technology* 2009; 2(2): 319–323.
20. Hebestreit P, Weng A, Bachran C, *et al.* Enhancement of cytotoxicity of lectins by Saponinum album. *Toxicon* 2006; 47(3): 330–335.
21. Datar RH, Richard JC. *Nanomedicine: Concepts, status and the future.* *Medical Innovation & Business* 2010; 2(3): 6–17.
22. Han G, Ghosh P, Rotello VM. Functionalized gold nanoparticle for drug delivery system. *Nanomedicine* 2007; 2: 113–123.
23. Jain PK, El-Sayed IH, El-Sayed MA. Au nanoparticles target cancer. *Nanotoday* 2007; 2: 18.
24. Mukherjee P, Pathangey LB, Bradley JB, *et al.* MUC1-specific immune therapy generates a strong anti-tumor response in a MUC1-tolerant colon cancer model. *Vaccine* 2007; 25(9): 1607–1617.
25. Singh AK, Tripathi YB, Pandey N, *et al.* Enhanced anti-lipopolysaccharide (LPS) induced changes in macrophage functions by *Rubia cordifolia* (RC) embedded with Au nanoparticles. *Free Radical Biology and Medicine* 2013; 65: 217–223.
26. Prawat U, Tuntiwachwuttikul P, Taylor WC. Steroidal saponins of *Costus lacerus*. *Science Asia* 1989; 15: 139–147.
27. Pina EML, Araújo FWC, Souza IA, *et al.* Pharmacological screening and acute toxicity of bark roots of *Guettarda platypoda*. *Revista Brasileira de Farmacognosia* 2012; 22(6): 1315–1322.
28. Firdhouse MJ, Lalitha P, Sripathi SK. An undemanding method of synthesis of gold nanoparticles using *Pisonia grandis* (R.Br.). *Digest Journal of Nanomaterials and Biostructures* 2014; 9: 385–393.
29. Fang J, Chen X, Liu B, *et al.* Liquid-phase chemoselective hydrogenation of 2-ethylanthraquinone over chromium-modified nanosized amorphous Ni-B catalysts. *Journal of Catalysis* 2005; 229: 97–104.
30. Parida UK, Bindhani BK, Nayak P. Green synthesis and characterization of old nanoparticles using onion (*Allium cepa*) extract. *World Journal of Nanoscience and Engineering* 2011; 1: 93–98.
31. Elia P, Zach R, Hazan S, *et al.* Green synthesis of gold nanoparticles using plant extracts as reducing agents. *International Journal of Nanomedicine* 2014; 9: 4007–4021.
32. Baker S, Satish S. Biosynthesis of gold nanoparticles by *Pseudomonas veronii* AS41G inhabiting *Annona squamosa* L. *Spectrochimica Acta Part A: Molecular and Bimolecular Spectroscopy* 2015; 150: 691–695.